Interaction estimation of pathogenicity determinant protein βC1 encoded by Cotton leaf curl Multan Betasatellite with *Nicotiana benthamiana* Nuclear Transport Factor 2

Ammara Nasim[1], Muhammad Abdul Rehman Rashid[1*], Khadim Hussain[1,2], Ibrahim Muhammad Al-Shahwan[2], Mohammed Ali Al-Saleh[2],

[1]Department of Bioinformatics and Biotechnology, Government College University Faisalabad, Pakistan

[2]Plant protection department, College of Food Sciences and Agriculture, King Saud University Riyadh 11451, Saudi Arabia

*Corresponding Author:
Muhammad Abdul Rehman Rashid,
Department of Bioinformatics and Biotechnology, Government College University Faisalabad, Pakistan
Email address: marrashid@gcuf.edu.pk,

Abstract

Background: Begomovirus is one of the most devastating pathogens that can cause more than 90% yield loss in various crop plants. The pathogenicity determinant βC1, located on the betasatellite associated with monopartite begomoviruses, alters the host signaling mechanism to enhance the viral disease phenotype by undermining the host immunity. The understanding of its interacting proteins in host plants to develop disease symptoms such as curly leaves, enations, vein swelling, and chlorosis is crucial to enhance the disease resistance in crop plants. The current study was designed to reveal the contribution of βC1 in disease pathogenicity and to unveil potential interacting partners of βC1 protein in the model plant *Nicotiana benthamiana.*

Methods: βC1 gene was cloned in pGKBT7 and used as bait against the cDNA library of *N. benthamiana* and its pathogenesis was tested against the healthy plant and the plants infiltrated with empty vectors. The yeast two-hybrid-based screening was performed to find the interacting factors. Successful interacting proteins were screened and evaluated in various steps and confirmed by sequence analysis. The three-dimensional structure of the Nuclear Transport Factor2 (NTF2) protein was predicted, and *in-silico* protein-protein interaction was evaluated. Furthermore, protein sequence alignment and molecular phylogenetic analysis were carried out to identify its homologues in other related families. *In-silico* analyses were performed to validate the binding affinity of βC1 protein with NTF2. The 3D model was predicted by using I-TASSER

38 and then analyzed by SWISS MODEL-Workspace, RAMPAGE, and Verify 3D. The interacting
39 amino acid residues of βC1 protein with NTF2 were identified by using PyMOL and Chimera.
40 **Results:** The agroinfiltrated leaf samples developed severe phenotypic symptoms of virus
41 infection. The yeast-two-hybrid study identified the NTF2 as a strong interacting partner of the
42 βC1. The NTF2 in *Solanaceae* and *Nicotiana* was found to be evolved from the *Brassica* and
43 *Gossypium* species. The *in-silico* interaction studies showed a strong binding affinity with
44 releasing energy value of -730.6 KJ/mol, and the involvement of 10 amino acids from the middle
45 portion towards the C-terminus and five amino acid residues from the middle portion of βC1 to
46 interact with six amino acids of NTF2. The study not only provided insight into the molecular
47 mechanism of pathogenicity but also put the foundation stone to develop the resistance
48 genotypes for commercial purposes and food security.
49 **Keywords:** CLCuMB, βC1, DNA satellites, Protein-protein interaction, Yeast two hybrid
50

Introduction

52   Plant viruses cause significant damage to the quality and production of crops. They pose
53 a severe risk to food security across the several places worldwide (Oerke & Dehne 2004).
54 Among the Plant viruses, *Geminivirus* from the *Geminivirdae* family is one of the largest groups.
55 According to the international committee on taxonomy of viruses (ICTV) classification, the family
56 *Geminivirdae* has evolved to divided into fourteen genera based on genome organization, insect, vectors,
57 and host range (Fiallo-Olivé et al. 2021). *Begomovirus* is the largest and economically most
58 important genus of all. Begomoviruses cause more than 90% yield loss in agronomic crops,
59 including cotton and tobacco (Brown et al. 2015). Cotton leaf curl Multan virus (CLCuMuV) is a
60 monopartite begomovirus (Yousaf et al. 2013). Monopartite begomoviruses are transmitted by
61 whitefly, and their genomes contain one circular, single-stranded DNA (ssDNA) (Anwar et al.
62 2020; Briddon et al. 2018; Mansoor et al. 2008). Besides, they contain an additional single-
63 stranded DNA, approximately 1,350 nucleotides in size, known as a betasatellite, involved to
64 promote the disease symptoms. The acquisition of new proteins and the integrating partners are
65 the common causes of viral genome evolution (Garamszegi et al. 2013). Hence, information
66 about virus-host interacting partners is required to understand the evolution of the viral genome
67 and for disease management.
68   The betasatellite belongs to the genus *Betasatellite*, consisting of 61 well-recognized
69 species, replicates and spreads through helper begomovirus (Nawaz-ul-Rehman et al. 2021). All
70 the betasatellites encode a multi-functional pathogenicity determinant, the *Beta C1 (*βC1)
71 protein, and the βV1 to induce the disease symptoms (Hu et al. 2020). The highly conserved βC1
72 gene, located on the complementary strand of betasatellite, is involved in the reprogramming of
73 host cellular processes to facilitate the begomoviruses-based infections (Li et al. 2018). It causes
74 pathogenicity by contributing to disease symptoms such as vein thickening, stunting, leaf
75 deformation, enation, and suppressing gene silencing (Amin et al. 2011; Khan et al. 2017; Yang
76 & Zhou 2017).

βC1 is reported to interact with many host factors to manipulate the infection and disease symptoms. After infection, βC1 moves to the nucleus of the infected plant cells and interacts with transcription factors to reprogram the gene expression, hence promoting viral propagation and disease symptoms (Hanley-Bowdoin et al. 2013). βC1 alters the expression levels of photosystem proteins, resulting a decrease in photosynthesis rate, which is one of the key reasons for developing disease symptoms in plants (Gnanasekaran et al. 2019; Sehrish et al. 2014). The aforementioned studies have clearly shown that βC1 has been playing a significant role in viral pathogenesis, leading to the initiation of the disease symptoms such as chlorosis, witling, and leaf deformation.

Coordination and regulation of cellular events in a eukaryotic cell depend on the transport of micro- and macro-molecules across the nucleus. Passive transport processes such as diffusion enable micro-molecules (40kDa) to move across the nuclear envelope (NE). The bigger molecules, on the other hand, cannot diffuse through the NE and hence require the assistance of other proteins in their active transport to the nucleus (Macara 2001; Paschal & Gerace 1995). The Nuclear Transport Factor 2 (NTF2) and GTP binding or RAs-related nuclear protein (Ran-proteins) are the two crucial soluble cytosolic factors that assist in active transport through permeabilized cells. To perform this function in nuclear transport, NTF2 interacts with the cytosolic factor Ran. In each transport cycle, Ran delivers one molecule to the cytoplasm which converts to the GTP-bound state and ultimately returns to the nucleus. As Ran is a small protein to diffuse through the nuclear pores, it results in low passive diffusion rate than that required for efficient nucleocytoplasmic traffic. To maintain the asymmetric cellular distribution of regulatory proteins, a small homodimeric protein NTF2 receives the signals and triggers the downstream signaling pathways. It binds specifically the GDP-bound and interacts with nuclear pore complexes (NPC) (Bayliss et al. 2002; Quimby et al. 2000; Ribbeck et al. 1998; Wong et al. 1997). Begomoviruses which replicate in the nucleus of the host may exploit this transport system for the movement of the virus genome from cytoplasm to nucleus. Despite the potential biological function suggested by earlier investigations, less was known about NTF2's contribution to plant defence against pathogen assault. *Nicotiana benthamiana (N. benthamiana)* has attained scientific importance due to its widespread usage as an experimental host plant as its genome data availability and successful inoculation of viral infection are helpful for scientific study (Goodin et al. 2008; Park et al. 2009). The *N. benthamiana* bears the special ability to be vulnerable to a wide range of plant viruses. As a result, it has emerged as a keystone for virus interaction studies.

The current study was designed to reveal the contribution of βC1 to disease pathogenicity and its interacting partner in the host plant *N. benthamiana*. To identify host factors interacting with CLCuMuB βC1, *N. benthamiana* GAL4-based yeast-two-hybrid (Y2H) approach developed by Fields & Song (Fields & Song 1989) was used to screen the cDNA library. This protein-protein interaction (PPI) was further evaluated using computational analysis. Identification of βC1 interacting host proteins will broaden the horizon of understanding virus-host interactions required for disease dissemination. Furthermore, the identification of βC1 interacting partners

117 would be helpful in the future to uncover the pathways involved in disease that could be
118 engineered to improve the plants' resilience against ever-evolving viruses.
119

Materials and Methods

Sequence retrieval for βC1and construction of expression cassette

122   Full-length βC1 gene was amplified from the isolate H181 of CLCuMB using the primers
123 having restriction sites HindIII and BamHI (F: CCAAGCTTATGACAACGAGCG and R:
124 CCGGATCCTTAAACGGTGAACT). The polymerase chain reaction (PCR) profile was
125 adjusted as an initial denaturation at 95°C for 5 min, denaturation at 95°C for 30 sec, annealing at
126 50°C for 30 sec, extension at 72°C for 30 sec and then final extension at72°c for 10 min followed
127 by 35 cycles.
128   The amplified product of βC1 (357 bps) was phenol-chloroform purified and digested to
129 clone under CaMV (Cauliflower Mosaic Virus) 35S promoter of expression vector pJIT-163.
130 Positive clones were confirmed by restriction analysis and further confirmed by standard PCR.
131 Gene expression cassette (1888 bps) was excised from positive clone samples in pJIT-163 vector
132 using SacI and XhoI. This expression cassette was cloned in binary vector pGreen-0029 at the
133 SacI and XhoI sites.

Agroinfiltration of expression cassette of βC1 gene

135   For in-planta interaction evaluation, *N. benthamiana* plants were grown under controlled
136 conditions including 16 hours of light, 8 hours of dark photoperiod at 28°C and 25°C day and
137 night temperature and approximately 65% humidity. Seeds of plants were grown in pots
138 containing peat moss for three weeks.
139   The expression cassette of βC1 gene and empty vector pGreen-0029 was electroporated
140 into *Agrobacterium tumefaciens* strain GV3101 within electroporation cuvette of (2mm space)
141 according to the previously reported procedure (Shen & Forde 1989). *Agrobacterium* culture
142 nurtured this construct of expression cassette and mock inoculation (empty vector pGreen-0029)
143 was grown within 100 µl of kanamycin and 25 µl of ampicillin per 100 ml media for 48 h (at
144 28°C). Bacterial cells were pelleted (5,000×g for 15 minutes at 4 °C) on an OD at 600nm of 1 and
145 then resuspended in 10 mM MgCl$_2$ and 100 µM acetosyringone. Cells were left for 2 to 3 h
146 before infiltration at room temperature. The *Agrobacterium* suspension was then infiltrated using
147 1 ml needle-free disposable syringe on the lower side of three weeks old healthy, young, and
148 fully expanded leaves directly. After infiltration, plants were placed in control conditions of 16 h
149 light photoperiod at 25°C to 28°C in an insect-free chamber.

Generating a Bait clone

151   Bait vector was constructed for Yeast-two-Hybrid analysis, primers designed having
152 restriction sites NcoI and BamHI (F: 5' AACC ATG GAA ATG ACA ACG AGC GGA ACA
153 and R: 5' CCG GAT CCT TAA ACG GTG AAC TTT TTA). The primers were designed to
154 avoid any codon change and frame-shift mutation. βC1 was amplified using these primers. The
155 conditions for PCR using Phusion High-Fidelity DNA polymerase (New England Biolabs,
156 Ipswich, MA, USA) with the following parameters: 98°C pre-denaturation temperature for 30

157 sec, denaturation at 98ºC for 10 sec: annealing at 55ºC for 30 sec: extension at 72ºC for 60 sec
158 following 35 cycles. A final extension was 72ºC for 7 minutes and hold temperature 25ºC. The
159 amplified DNA fragment of βC1 was cloned into the vector pGBKT7 (Clontech Laboratories
160 Inc., Mountain View, CA, USA), It has a GAL4 DNA-binding domain, Kanʳ for *Escherichia coli*
161 selection, and *TRP1* for yeast selection. As a result, the gene encoding for βC1 was included in
162 the pGBKT7 vector, which was created as bait for a GAL4-based two-hybrid system and given
163 the name as pGBKT7-βC1.Y2H Gold cells were transformed with 100ng of pGBKT7-βC1
164 construct along with positive and negative control, whereas, pGBKT7-53 was a positive control
165 and pGBKT7-lam was used as the negative control. Preparation of master mix by using
166 denatured salmon sperm DNA (ssDNA) at 100°C for 5 min, 50% PEG and 1M Lithium Acetate
167 [LiAC] was done. The mixture was heated at 30°C for 30 min, 42°C for 20 min, and cool the
168 tubes on ice for 10 min. 100µL of transformants was spread on a single SD/-Trp plate while
169 spreading of positive and negative was done on SD/-Leu/-Trp plates. Bait autoactivation and
170 toxicity test were done by transforming pGBKT7-βC1 construct into Y2H Gold cells along with
171 positive and negative controls.

172 **Screening of βC1 interacting partner**

173 The *N. benthamiana* cDNA library was generated with an activation domain (AD)
174 having GAL4-AD (Clontech Laboratories Inc., Mountain View, CA, USA). It was generated at
175 Plant Virology Lab at The University of Arizona, USA. Concentrated bait culture of pGBKT7-
176 βC1 working as binding domains (BD) was prepared and combined with library vial AD, after
177 mating the culture was spread on an array of selective agar plates. Initially on 150mm double
178 dropout SD/–Leu/–Trp (DDO), Quarter dropout SD/-Ade/His/Leu/-Trp QDO/X- α-Gal agar
179 plates following incubation at 30°C for 3-5 days.

180 Mating efficiency was determined by the following formula:

181 Mating efficiency (Diploids %) $= \dfrac{\text{Number of cfu/ml of diploids}}{\text{Number of cfu/ml of limiting partner}} \times 100$

182 Whereas, the number of colony forming units per mL (cfu/mL) of diploid indicated the Diploid
183 viability that was equal to number of cfu/mL on SD/–Leu/–Trp, Number of cfu/mL of limiting
184 partner was estimated as viability of the Prey Library that was equal to the number of cfu/mL on
185 SD/–Leu, while the viability of Bait was equal to the number of cfu/mL on SD/–Trp.

186 **Confirmation of positive interaction and rescuing prey plasmid**

187 The true positive prey plasmids were rescued from a single blue colony selected from
188 Y2H experiment and re-streaked on DDO/X- α-Gal agar plates (Table 1). The cultures were
189 inoculated overnight in DDO medium at 30°C. The plasmids were isolated from yeast cells and
190 used for transformation into *E. coli* DH5α cells. Plasmids showed positive interaction was further
191 evaluated and confirmed by transformation and co-transformation.

192 **Prey plasmid PCR for sequencing**

193 Ten samples showing genuine positive interaction were used for sequence analysis.
194 Plasmids isolated from yeast cells were used for PCR (Table 2). The PCR amplicons were
195 analyzed on 1% Agarose gel. The positive clones were confirmed by amplification with SMART
196 III primer and CDS III primer from both directions (Table 2).

Sequence homology, alignment, and evolution analyses

NTF2 gene sequence and protein sequences were subjected to the Basic Local alignment search tool for nucleotides (BLASTN) for the identification of their close relatives. Multiple sequence alignments were performed to construct the neighbor-joining phylogenetic tree using MEGA7 (Kumar et al. 2016) and sequence pairwise identity was analyzed by the Clustal W algorithm in MegAlign application Lasergene package of sequence analysis software (DNA Star Inc., Madison, WI, USA).

Protein structure prediction of viral proteins

The protein structure of NTF2 was retrieved from the National Center of Biotechnology Information (NCBI) database (XP_019236968). Evaluation of primary protein structure including the amino acid composition, atomic composition, molecular weight, theoretical isoelectric point (p*I*), estimated half-life, extinction coefficient, instability index, aliphatic index, and grand average of hydropathicity (GRAVY) was determined by using ProtParam (https://web.expasy.org/protparam/) (Gasteiger et al. 2005). PSIPRED tools were used for secondary protein structure analysis (http://bioinf.cs.ucl.ac.uk/psipred/). As Protein Data Bank (PDB) did not have a three-dimensional (3D) structure of the NTF2 protein, therefore, I-TASSER online server (https://zhanglab.ccmb.med.umich.edu/I-TASSER/) (Zhang 2008) was used for 3D structure prediction. Then, the model was further refined by using ModRefiner (https://zhanglab.ccmb.med.umich.edu/ModRefine/). After 3D model prediction and refinement of the NTF2, further structural evaluation, validation, and stereo-chemical analysis were performed. Evaluation of backbone confirmation was done by examining the ψ/φ Ramachandran plot acquired from RAMPAGE (http://mordred.bioc.cam.ac.uk/~rapper/rampage.php) (Lovell et al. 2003). The 3D model was assessed by Verify-3D (http://servicesn.mbi.ucla.edu/Verify3D/) to determine three-dimensional protein profiles and compatibility of the atomic model with its own amino acid sequence in comparison to the results of good structure (Eisenberg et al. 1997).

Protein-protein interaction (PPI) evaluation

A web-based server ClusPro 2.0 (https://cluspro.bu.edu), was used to perform Protein-Protein interaction analysis. It performs rigid-body docking of two proteins by giving a basic interface and gives the lowest energy of an interacting complex. ClusPro 2.0 required only two pdb files, receptor, and ligand (Comeau et al. 2004). βC1 model was used as a receptor, while predicted NTF2 was used as a ligand. Furthermore, PyMOL v1.7.4 software and Chimera (DeLano 2002) were used to visualize and analyze the interactions between receptor and ligand complexes, thus obtained.

Results

Transient expression of 35S-βC1 from CLCuMB strain in model host plant *Nicotiana benthamiana*

Non-transgenic *N. benthamiana* plants were inoculated with *Agrobacterium* cultures harboring expression cassette of βC1 gene from CLCuMB strain and analyzed the infectivity and symptoms induction ability of 35S-βC1 gene expression cassette. Inoculated leaves sample developed severe phenotypic symptoms of virus infection at 14 days post-inoculation (dpi). The

237   health plants (Fig. 1A) and the plants inoculated with empty vector (Fig. 1B) were compared to
238   the agroinfiltrated plants (Fig. 1C). These symptoms were downward leaf curling and yellowing
239   of inoculated leaves area were observed on the infiltrated leaves (Fig. 1C). With the passage of
240   time, the symptoms became prominent and deeply intense. In all of the four inoculated *N.*
241   *benthamiana* plants, the leaf showed these typical symptoms at 21-25 dpi when compared to
242   control leaves infiltrated with empty vector pGreen-0029 and healthy plants (Fig. 1A and 1B).
243   The appearance of infectious symptoms in all the nurture leaves confirmed the working
244   efficiency of the 35S-βC1 construct in the model plants and justified the major role of the βC1
245   gene in diseased symptoms induction in infected plants.

246 **Yeast two hybrid assay using βC1 as bait and *N. benthamiana* proteins as prey**

247   Based on the available virus genome sequence information (Accession No. LN886545.1),
248   primers for the βC1 gene were designed. βC1 was cloned into the pGBKT7 vector and confirmed
249   by sequencing showing no point mutation. The results showed 100% identity with the βC1 gene
250   encoded by CLCuMB. Transformation for confirmed clones was done into Y2H Gold competent
251   cells.

252   A preliminarily study for the autoactivation of βC1 was conducted to investigate the
253   interaction among bait and prey fusion proteins. Yeast cells expressing the reporter genes *HIS3*
254   and *His3* auxotrophic on histidine deficient medium were employed for verification. No growth
255   was observed in yeast cells when pGBKT7-βC1construct was co-expressed with pGADT7-
256   empty in the histidine-deficient medium. In contrast, positive control showed blue colonies
257   indicating that there was a positive interaction between 53+t, similarly, negative control lam+t
258   showed no interaction at all (Fig. 2).

259   For mating, the screening of more than 2×10^7 cells per mL was confirmed by library
260   tittering. Mating efficiency was 5.6% which was sufficient to screen the library successfully
261   (Table 3). Positively interacted proteins showing blue colonies from 150 mm DDO/ X-α-Gal
262   plates were further screened and purified by patching on DDO/ X-α-Gal plates and QDO/ X-α-
263   Gal agar plates (Fig. 3). Positive interacted protein's plasmids were rescued by transformation
264   into *Dh5α* of *E. coli.*

265 **Validation of positive interaction through transformation and co-transformation**

266   After being propagated in *E. coli*, the extracted plasmids were again transformed into
267   yeast and co-expressed with the pGBKT7-βC1 construct to examine the reproducibility of the
268   candidate proteins in retransformed yeast cells. On SD/Leu-/Trp-/His- plates, yeast transformants
269   were dispersed, and the survival rate was used to assess the interaction's efficacy. Positive clones
270   were further verified to have strong positive interaction by spreading onto SD/Leu–/Trp–/His–
271   /Ade– plates. As a final point, ten positive clones with strong βC1 interacting proteins were
272   identified.

273 **Identification of *in vivo* βC1 interacting proteins using Y2H**

274   Ten candidate protein plasmids showing genuine positive interaction were-sequenced for
275   further analyses (Supplementary Table 1). The sequencing data was validated for true interaction
276   by homology study, sequence alignment, and open reading frames (ORFs) detection. The

277 sequence homolog was searched in NCBI by the BLASTN tool. All the identified sequences
278 were translated, a significant chunk of sequences was revealed, and ORFs were extracted and
279 aligned. Finally, the similarity index was estimated by the BLAST tool of NCBI. Among the
280 identified sequences, the LOC109217199 mRNA of *Nicotiana tabacum* nuclear transport factor
281 2-like occurred repeatedly. Therefore, the sequences encoding for Nuclear Transport Factor-2
282 occurring more than once indicated the best interacting partner of βC1 protein.

283 Phylogenetic analysis of NTF2 encoded genes and encoded proteins

284 Gene sequences of NTF2 from *N. benthamiana* and other plant species were aligned to
285 find its close relatives. Twenty closely related sequences were retrieved from databases with the
286 help of BLASTN. In phylogenetic analysis of *N. benthamiana* NTF2 sequence showed the
287 closest relationship with the members of its own genus *Nicotiana tabacum* and *Nicotiana*
288 *attenuata*. Next closest clade of NTF2 gene sequences consisted of *Solanum tuberosum* (potato),
289 *Solanum lycopersicum* (tomato) from the genus *Solanum* of the Solanaceae family (Fig. 4,
290 Supplementary Table 2).

291 In phylogenetic analysis, the studied NTF2 protein sequence also showed the closest
292 relationship with same members of its own genus *Nicotiana* as revealed for gene sequence.
293 Further, the NTF2 protein sequence was rooted to the *Brassica rapa* (Turnip) and *Arabidopsis*
294 family suggesting the wide pedigree of NTF2 from these species (Fig. 5, Supplementary Table
295 3).

296 *In silico* prediction of viral protein structure

297 The NTF2 data retrieved from the online server revealed 123 amino acid residues. Its
298 primary structure showed a molecular weight of 13747.67 Dalton, and a 5.87 p*I*-value (Fig 6A).
299 The p*I* value was below 7, which indicated the negatively charged protein. Significant stability of
300 protein was revealed by computed instability index of 39.37. The availability of methionine (M)
301 at the N-terminus of the protein, and the negative large average of hydropathicity (-0.089)
302 indicated that the protein was hydrophobic in nature. The Glutamine (Q), Leucine (L), Glycine
303 (G), Phenylalanine (F), Serine (S), and Valine (V) residues were observed in excess (Fig 6A).

304 Secondary structure analysis exposed that NTF2 had 20.32% helices and 29.26%
305 extended strands (β-sheets) (Fig 6B). The predicted 3D model of NTF2 (Fig 6C) was also
306 evaluated through the Ramachandran plot. The 96.7% of the residues were found in the favored
307 region, 2.5% of the residues were in the allowed region and only 0.8% residues were found in the
308 outlier region (Fig 6D). I-TASSER was used to predict the 3D structure of NTF2 and the
309 predicted structure was refined by ModRefiner. Having more than 99% residues of the predicted
310 structure in the favored and allowed regions, the structure was considered to be validated (Fig
311 6E).

312 Estimation of protein-protein interaction (PPI)

313 To study the PPI of βC1 and NTF2, βC1 protein was used as a receptor in cluspro while
314 NTF2 was used as the ligand (Fig 6F). Interaction studies of βC1 with NTF2 showed a strong
315 binding affinity with releasing energy value of -730.6 KJ/mol (Table 4). Analysis of interacting
316 residues showed that 10 amino acids from the middle portion towards the C-terminus and five

317 amino acid residues (TYR48, TYR50, ASP52, ASP58, ASN60) from the middle portion of βC1
318 interacted with six amino acids of NTF2 (Table 4).

319   **Discussion**DNA betasatellites associated with helper mono-, and bi-partite
320 begomoviruses depend on the begomoviruses for their replication encapsidation, and spread
321 (Fiallo-Olivé & Navas-Castillo 2020). The satellites contribute to the helper virus's symptomatic
322 range (Briddon & Stanley 2006). Betasatellites consist of a single complementary sense gene
323 (βC1), an adenine-rich region (A-rich region), and a satellite-conserved region (Briddon et al.
324 2003). The βC1, a pathogenicity determinant and suppressor of PTGS, up-regulates viral DNA
325 levels, binds DNA and RNA, and facilitates the virus intracellular movement in plants (Hu et al.
326 2020; Li et al. 2018; Nair et al. 2020; Saeed et al. 2007). βC1 interacts with the host plant
327 machinery for the successful propagation of disease (Kamal et al. 2019b).
328 During an infection cycle, viruses direct many changes in the intracellular environment of the
329 host cell and provide a safe passage to spread a successful infection by circumventing the
330 antiviral defense mechanism. For the last few decades, virology just focused on the pathogen, but
331 now it is believed that knowing "the host response" is equally or more important in determining
332 the pathological outcome of infection (Peng et al. 2009). Virus-host interaction studies are a
333 helpful tool to understand how viruses manipulate host machinery and cause disease. Biological
334 data retrieval and *in-silico* analyses provide an understanding of new hosts which potentially associated
335 with CLCuD viruses/satellites but lack the information of binding sites (Kamal et al. 2019a).

336

337   In this study, we identified NTF2 as a strong interacting partner of CLCuMB βC1 by
338 screening a *N. benthamiana* Y2H library with the βC1 as a bait. This interaction was evaluated
339 and validated using the *in-silico* analysis of the protein-protein interaction. Many recent studies
340 used Y2H and transcriptomics approaches to understand the interactional pathways of viruses
341 with host plants (Kamal et al. 2019a; Liu et al. 2014).

342   The NTF2 is involved in the nuclear transportation of macromolecules. Mostly the viral
343 proteins or plant viruses interact with the chloroplast proteins to aid viral infection and disease
344 symptoms induction (DeBlasio et al. 2018; Kong et al. 2014). The NTF2, a protein involved in
345 nuclear trafficking, is conserved in most of the eukaryotes including, yeast, mammals, and
346 *Arabidopsis*. It shows a diverse biological function in different species. Changes in its mRNA
347 expression in various stress conditions depict its involvement not only in normal protein
348 translocation but also in the regulation and mitigation of challenges posed by deleterious
349 conditions (Quimby et al. 2000).

350   This is the first report of the interaction between NTF2 and βC1 protein of the
351 betasatellites. However, other viral proteins have been reported to interact with plant NTF2. For
352 instance, ectopic higher expression of *Arabidopssi NTF2* in *N. benthemiana* results in impaired
353 translocation of a transcription factor and GTPases (Zhao et al. 2006). In addition, it expresses at
354 a higher rate in soybean roots challenged with *Meloidogyne javanica* (Sá et al. 2012).
355 Furthermore, *ntf2* knockdown wheat lines showed more susceptibility to stripe rust, a disease
356 caused by *Puccinia striiformis,* suggesting a positive role of NTF2 in plant immunity (Zhang et
357 al. 2018).

358   The interaction of NTF2 and βC1 was evidenced using further expression of βC1 in *N.*
359   *benthamiana.* βC1was transiently expressed in the *N. benthamiana* leaves. The expression of
360   βC1induced typical symptoms in the infected agroinfiltrated leaves like chlorosis, leaf witling,
361   and deformation. In host-virus interactions, the offending pathogen frequently develops counter-
362   defense tactics to a host's defensive mechanisms (Sheikh 2018). The presence of upward-curled
363   leaves or even radial leaves in agroinfiltrated plants suggested that this viral pathogenic protein
364   may disrupt the formation of adaxial–abaxial polarity in leaves (Wang et al. 2015). The *N.*
365   *benthamiana* leaves carrying pGreen-βC1, pGreen-empty and healthy-control plants in this study
366   showed different levels of protein expression (Fig 1). The typical symptoms of leaf deformation
367   were clearly observable in leaves carrying the pGreen-βC1 (Fig 1C), while there was no
368   expression on leaves with an empty vector and the control-healthy plant (Fig 1A & 1B). These
369   findings not only validated the integration and proper working of βC1 in *N. benthamiana* but
370   also described the interaction of the viral protein with the host plant machinery to evade host
371   defense mechanism.
372   Phylogenetic analysis was carried out to evaluate the conservation of NTF2 in different
373   species (Supplementary Table 2 and 3). The NTF2 gene of *N. benthaminia* in the current study
374   showed the closest relationship and the highest sequence identity with the NTF2 gene in the *N.*
375   *tabacum* and *N. attenuata* (Fig 4 and 5). The previous studies showed that geminiviruses caused
376   different diseases in *Nicotiana tabacum* and *Nicotiana sylvestris* (Murad et al. 2004). The
377   background relationship with *Solanum lycopersicum,* and the sequence identity with different
378   members of the genus Gossypium was further elaborated in results. The literature revealed that
379   the members of geminivirus actively target the species of genus Solanum and Gossypium, and
380   induce curly leaf symptoms and leaf deformation (Naqvi et al. 2017; Prajapat et al. 2013; Varma
381   & Malathi 2003). The NTF2 from the *Capsicum annum* showed its conversation with NTF2 of
382   *N. benthaminia*. The yellow leaf curl disease in the genus capsicum has also been reported by
383   begomovirus caused (Mishra et al. 2020). High gene and protein sequence identity indicate the
384   NTF2 homologs' presence in a wide range of host plant families. It is involved in disease
385   development by interaction with βC1 protein. The homology and conservation of NTF2 is not
386   only proved in plants but also in yeast and mammals along with elaboration of its function in
387   targeting proteins into the nucleus (Bhattacharya & Steward 2002). Furthermore, it was
388   determined that the sequences of NTF2 in yeast, humans, and Arabidopsis were noticeably
389   similar(Zhao et al. 2006).
390   *In silico* protein-protein docking results of this study depicted the strong interaction
391   between NTF2 and viral protein CLCuMB βC1, which was further substantiated by Y2H assays.
392   Overall, the current study found that NTF2 had a strong binding affinity with βC1 as indicated
393   by the involvement of six residues with the lowest energy value of -730.6KJ/mol. So, suggesting
394   its potential role in nuclear trafficking of begomovirus genome, its replication, and dissemination
395   in neighboring cells can cause chlorosis, leaf curling, and/or witling symptoms. Various multi-
396   pronged *in-silico* techniques on the basis of energetic, sequence conservation analysis, and the

397 binding site might be useful to envisage the host-pathogen interaction such as geminivirus
398 proteins and their interacting partners in cotton (Kamal et al. 2019a).

Conclusion

400 This study aimed to evaluate the pathogenicity of βC1 protein and its interacting partners.
401 The agroinfiltrated leaves of *N. benthamiana* showed the disease symptoms as chlorosis and leaf
402 deformation. We proposed a new role for βC1 in plant immunity responses that has been in veil
403 until now. The Y2H-based experiment and *in-silico* protein analyses presented in the current
404 study suggested that the βC1 strongly interacts with NTF2, for nuclear transportation. Further
405 studies on βC1 tagging with the green fluorescent protein (GFP) in wild-type and *ntf2* mutant
406 background will shed light on the NTF2 requirement for its nuclear translocation and disease
407 propagation. In the future, the interaction site mapping and mutant studies will aid in finding the
408 NTF2 domain involved in interaction with βC1. Finding interaction sites will pave the way to
409 find the common mechanism involved in βC1 nuclear translocation in many host plants. The
410 results in this study may not only provide an insight into resistance mechanism but also set a
411 base for future research on the involvement of cytoplasmic nuclear transportation in protein
412 interaction and disease defense mechanisms.

Acknowledgment

414 We would like to acknowledge the School of Plant Sciences, University of Arizona, USA
415 for their assistance in providing the *N. benthamiana* "Mate and Plate" library.

References

418 Amin I, Hussain K, Akbergenov R, Yadav JS, Qazi J, Mansoor S, Hohn T, Fauquet CM, and
419   Briddon RW. 2011. Suppressors of RNA silencing encoded by the components of the
420   cotton leaf curl begomovirus-betasatellite complex. *Molecular plant-microbe interactions*
421   24:973-983.
422 Anwar I, Bukhari HA, Nahid N, Rashid K, Amin I, Shaheen S, Hussain K, and Mansoor S. 2020.
423   Association of cotton leaf curl Multan betasatellite and Ageratum conyzoides
424   symptomless alphasatellite with tomato leaf curl New Delhi virus in Luffa cylindrica in
425   Pakistan. *Australasian Plant Pathology* 49:25-29.
426 Bayliss R, Leung SW, Baker RP, Quimby BB, Corbett AH, and Stewart M. 2002. Structural
427   basis for the interaction between NTF2 and nucleoporin FxFG repeats. *The EMBO
428   journal* 21:2843-2853.
429 Bhattacharya A, and Steward R. 2002. The Drosophila homolog of NTF-2, the nuclear transport
430   factor-2, is essential for immune response. *EMBO reports* 3:378-383.
431 Briddon R, and Stanley J. 2006. Subviral agents associated with plant single-stranded DNA
432   viruses. *Virology* 344:198-210.
433 Briddon RW, Bull SE, Amin I, Idris AM, Mansoor S, Bedford ID, Dhawan P, Rishi N, Siwatch
434   SS, and Abdel-Salam AM. 2003. Diversity of DNA β, a satellite molecule associated
435   with some monopartite begomoviruses. *Virology* 312:106-121.
436 Briddon RW, Martin DP, Roumagnac P, Navas-Castillo J, Fiallo-Olivé E, Moriones E, Lett J-M,
437   Zerbini FM, and Varsani AJAov. 2018. Alphasatellitidae: a new family with two
438   subfamilies for the classification of geminivirus-and nanovirus-associated alphasatellites.
439   *Archives of virology* 163:2587-2600.

440   Brown JK, Zerbini FM, Navas-Castillo J, Moriones E, Ramos-Sobrinho R, Silva JC, Fiallo-Olivé
441   E, Briddon RW, Hernández-Zepeda C, and Idris A. 2015. Revision of Begomovirus
442   taxonomy based on pairwise sequence comparisons. Springer.
443   Comeau SR, Gatchell DW, Vajda S, and Camacho CJ. 2004. ClusPro: an automated docking and
444   discrimination method for the prediction of protein complexes. *Bioinformatics* 20:45-50.
445   DeBlasio SL, Rebelo AR, Parks K, Gray SM, and Heck MC. 2018. Disruption of chloroplast
446   function through downregulation of phytoene desaturase enhances the systemic
447   accumulation of an aphid-borne, phloem-restricted virus. *Molecular plant-microbe
448   interactions* 31:1095-1110.
449   DeLano WL. 2002. Unraveling hot spots in binding interfaces: progress and challenges. *Current
450   opinion in structural biology* 12:14-20.
451   Eisenberg D, Lüthy R, and Bowie J. 1997. VERIFY3D: assessment of protein models with three-
452   dimensional profiles. InMethods in enzymology. *Academic Press DOI* 10:396-404.
453   s0076-6879
454   Fiallo-Olivé E, Lett JM, Martin DP, Roumagnac P, Varsani A, Zerbini FM, and Navas-Castillo J.
455   2021. ICTV Virus Taxonomy Profile: Geminiviridae 2021. *J Gen Virol* 102.
456   10.1099/jgv.0.001696
457   Fiallo-Olivé E, and Navas-Castillo J. 2020. Molecular and Biological Characterization of a New
458   World Mono-/Bipartite Begomovirus/Deltasatellite Complex Infecting Corchorus
459   siliquosus. *Front Microbiol* 11:1755. 10.3389/fmicb.2020.01755
460   Fields S, and Song O-k. 1989. A novel genetic system to detect protein–protein interactions.
461   *Nature* 340:245-246.
462   Garamszegi S, Franzosa EA, and Xia Y. 2013. Signatures of pleiotropy, economy and
463   convergent evolution in a domain-resolved map of human–virus protein–protein
464   interaction networks. *PLoS pathogens* 9:e1003778.
465   Gasteiger E, Hoogland C, Gattiker A, Wilkins MR, Appel RD, and Bairoch A. 2005. Protein
466   identification and analysis tools on the ExPASy server. *The proteomics protocols
467   handbook*:571-607.
468   Gnanasekaran P, KishoreKumar R, Bhattacharyya D, Vinoth Kumar R, and Chakraborty S.
469   2019. Multifaceted role of geminivirus associated betasatellite in pathogenesis. *Mol Plant
470   Pathol* 20:1019-1033. 10.1111/mpp.12800
471   Goodin MM, Zaitlin D, Naidu RA, and Lommel SA. 2008. Nicotiana benthamiana: its history
472   and future as a model for plant–pathogen interactions. *Molecular plant-microbe
473   interactions* 21:1015-1026.
474   Hanley-Bowdoin L, Bejarano ER, Robertson D, and Mansoor S. 2013. Geminiviruses: masters at
475   redirecting and reprogramming plant processes. *Nature Reviews Microbiology* 11:777-
476   788.
477   Hu T, Song Y, Wang Y, and Zhou X. 2020. Functional analysis of a novel βV1 gene identified in
478   a geminivirus betasatellite. *Sci China Life Sci* 63:688-696. 10.1007/s11427-020-1654-x
479   Kamal H, Minhas F-u-AA, Farooq M, Tripathi D, Hamza M, Mustafa R, Khan MZ, Mansoor S,
480   Pappu HR, and Amin I. 2019a. In silico prediction and validations of domains involved
481   in Gossypium hirsutum SnRK1 protein interaction with cotton leaf curl Multan
482   betasatellite encoded βC1. *Frontiers in plant science*:656.
483   Kamal H, Minhas F-u-AA, Tripathi D, Abbasi WA, Hamza M, Mustafa R, Khan MZ, Mansoor
484   S, Pappu HR, and Amin I. 2019b. βC1, pathogenicity determinant encoded by Cotton leaf

485   curl Multan betasatellite, interacts with calmodulin-like protein 11 (Gh-CML11) in
486   Gossypium hirsutum. *PloS one* 14:e0225876.
487 Khan A, Fiaz S, Bashir I, Ali S, Afzal M, Kettener K, Mahmood N, and Manzoor M. 2017.
488   Estimation of genetic effects controlling different plant traits in cotton (Gossypium
489   hirsutum L.) under clcuv epidemic condition. *Cercetari Agronomice in Moldova*.
490 Kong L, Wu J, Lu L, Xu Y, and Zhou X. 2014. Interaction between Rice stripe virus disease-
491   specific protein and host PsbP enhances virus symptoms. *Molecular plant* 7:691-708.
492 Kumar S, Stecher G, and Tamura K. 2016. MEGA7: molecular evolutionary genetics analysis
493   version 7.0 for bigger datasets. *Molecular biology evolution* 33:1870-1874.
494 Li F, Yang X, Bisaro DM, and Zhou X. 2018. The βC1 Protein of geminivirus–betasatellite
495   complexes: a target and repressor of host defenses. *Molecular plant* 11:1424-1426.
496 Liu J, Yang J, Bi H, and Zhang PJJoIPB. 2014. Why mosaic? Gene expression profiling of
497   African cassava mosaic virus-infected cassava reveals the effect of chlorophyll
498   degradation on symptom development. *Journal of Integrative Plant Biology* 56:122-132.
499 Lovell SC, Davis IW, Arendall III WB, De Bakker PI, Word JM, Prisant MG, Richardson JS,
500   and Richardson DC. 2003. Structure validation by Cα geometry: ϕ, ψ and Cβ deviation.
501   *Proteins: Structure, Function, Bioinformatics* 50:437-450.
502 Macara IG. 2001. Transport into and out of the nucleus. *Microbiology molecular biology reviews*
503   65:570-594.
504 Mansoor S, Amin I, and Briddon RJEov. 2008. Cotton leaf curl disease. *Encyclopedia of
505   virology* 5:563-569.
506 Mishra M, Verma RK, Marwal A, Sharma P, and Gaur R. 2020. Biology and interaction of the
507   natural occurrence of distinct monopartite begomoviruses associated with satellites in
508   Capsicum annum from India. *Frontiers in microbiology* 11:2366.
509 Murad L, Bielawski J, Matyasek R, Kovarik A, Nichols R, Leitch A, and Lichtenstein C. 2004.
510   The origin and evolution of geminivirus-related DNA sequences in Nicotiana. *Heredity*
511   92:352-358.
512 Nair A, Chatterjee KS, Jha V, Das R, and Shivaprasad PV. 2020. Stability of Begomoviral
513   pathogenicity determinant βC1 is modulated by mutually antagonistic SUMOylation and
514   SIM interactions. *BMC Biology* 18:110. 10.1186/s12915-020-00843-y
515 Naqvi RZ, Zaidi SS-e-A, Akhtar KP, Strickler S, Woldemariam M, Mishra B, Mukhtar MS,
516   Scheffler BE, Scheffler JA, and Jander G. 2017. Transcriptomics reveals multiple
517   resistance mechanisms against cotton leaf curl disease in a naturally immune cotton
518   species, Gossypium arboreum. *Scientific Reports* 7:1-15.
519 Nawaz-ul-Rehman MS, Nahid N, Hassan M, and Mubin M. 2021. Betasatellites and
520   Deltasatelliles (Tolecusatellitidae). In: Bamford DH, and Zuckerman M, eds.
521   *Encyclopedia of Virology (Fourth Edition)*. Oxford: Academic Press, 239-246.
522 Oerke E-C, and Dehne H-W. 2004. Safeguarding production—losses in major crops and the role
523   of crop protection. *Crop protection* 23:275-285.
524 Park M-R, Park S-H, Cho S-Y, and Kim K-H. 2009. Nicotiana benthamiana protein, NbPCIP1,
525   interacting with Potato virus X coat protein plays a role as susceptible factor for viral
526   infection. *Virology* 386:257-269.
527 Paschal BM, and Gerace L. 1995. Identification of NTF2, a cytosolic factor for nuclear import
528   that interacts with nuclear pore complex protein p62. *The Journal of Cell Biology*
529   129:925-937.

530 Peng X, Chan EY, Li Y, Diamond DL, Korth MJ, and Katze MG. 2009. Virus–host interactions:
531   from systems biology to translational research. *Current opinion in microbiology* 12:432-
532   438.
533 Prajapat R, Marwal A, and Gaur RK. 2013. Evidence of the Association of Solanum leaf curl
534   lakshmangarh virus with a Weed Plant Solanum nigrum in Rajasthan, India. *Science
535   International* 1:379-383.
536 Quimby BB, Lamitina T, L'Hernault SW, and Corbett AH. 2000. The mechanism of ran import
537   into the nucleus by nuclear transport factor 2. *Journal of Biological Chemistry*
538   275:28575-28582.
539 Ribbeck K, Lipowsky G, Kent HM, Stewart M, and Görlich D. 1998. NTF2 mediates nuclear
540   import of Ran. *The EMBO journal* 17:6587-6598.
541 Sá MELd, Lopes MJC, Campos MdA, Paiva LV, Amorim RMSd, Beneventi MA, Firmino AAP,
542   and Sá MFGd. 2012. Transcriptome analysis of resistant soybean roots infected by
543   Meloidogyne javanica. *Genetics Molecular Biology* 35:272-282.
544 Saeed M, Zafar Y, Randles JW, and Rezaian MA. 2007. A monopartite begomovirus-associated
545   DNA β satellite substitutes for the DNA B of a bipartite begomovirus to permit systemic
546   infection. *Journal of General Virology* 88:2881-2889.
547 Sehrish M, Fakhra S, Muhammad S, and Haider MS. 2014. Effect of whitefly transmitted
548   Geminiviruses on the physiology of tomato (Lycopersicon esculentum L.) and tobacco
549   (Nicotiana benthamiana L.) plants. *Journal of Natural Sciences Research* 4:109-118.
550 Sheikh MA. 2018. Plant defense and counter defense by viruses. *Advances in Plant Pathology*:
551   IntechOpen.
552 Shen WJ, and Forde BG. 1989. Efficient transformation of Agrobacterium spp. by high voltage
553   electroporation. *Nucleic Acids Res* 17:8385. 10.1093/nar/17.20.8385
554 Varma A, and Malathi V. 2003. Emerging geminivirus problems: a serious threat to crop
555   production. *Annals of Applied Biology* 142:145-164.
556 Wang J, Yu W, Yang Y, Li X, Chen T, Liu T, Ma N, Yang X, Liu R, and Zhang B. 2015.
557   Genome-wide analysis of tomato long non-coding RNAs and identification as
558   endogenous target mimic for microRNA in response to TYLCV infection. *Scientific
559   Reports* 5:16946. 10.1038/srep16946
560 Wong DH, Corbett AH, Kent HM, Stewart M, and Silver PA. 1997. Interaction between the
561   small GTPase Ran/Gsp1p and Ntf2p is required for nuclear transport. *Molecular Cellular
562   Biology* 17:3755-3767.
563 Yang X, and Zhou X. 2017. Betasatellites of Begomoviruses. *Viroids and satellites*. Academic
564   Press, USA: Elsevier, 671-678.
565 Yousaf S, Rasool G, Amin I, Mansoor S, and Saeed M. 2013. Interference of a synthetic rep
566   protein to develop resistance against cotton leaf curl disease. *International Journal of
567   Agriculture Biology* 15.
568 Zhang Q, Wang B, Wei J, Wang X, Han Q, and Kang Z. 2018. TaNTF2, a contributor for wheat
569   resistance to the stripe rust pathogen. *Plant Physiology Biochemistry* 123:260-267.
570 Zhang Y. 2008. I-TASSER server for protein 3D structure prediction. *BMC bioinformatics* 9:1-8.
571 Zhao Q, Leung S, Corbett AH, and Meier I. 2006. Identification and characterization of the
572   Arabidopsis orthologs of nuclear transport factor 2, the nuclear import factor of ran. *Plant
573   physiology* 140:869-878.
574

Figure 1

The βC1 ORF expression evaluated by agrobacterium-infiltration

The disease-like symptoms in *Nicotiana benthamiana*. (A) is the healthy plant, (B) leaves infiltrated with empty vector, and (C) the leaves infiltrated leaves with pGreen-βC1
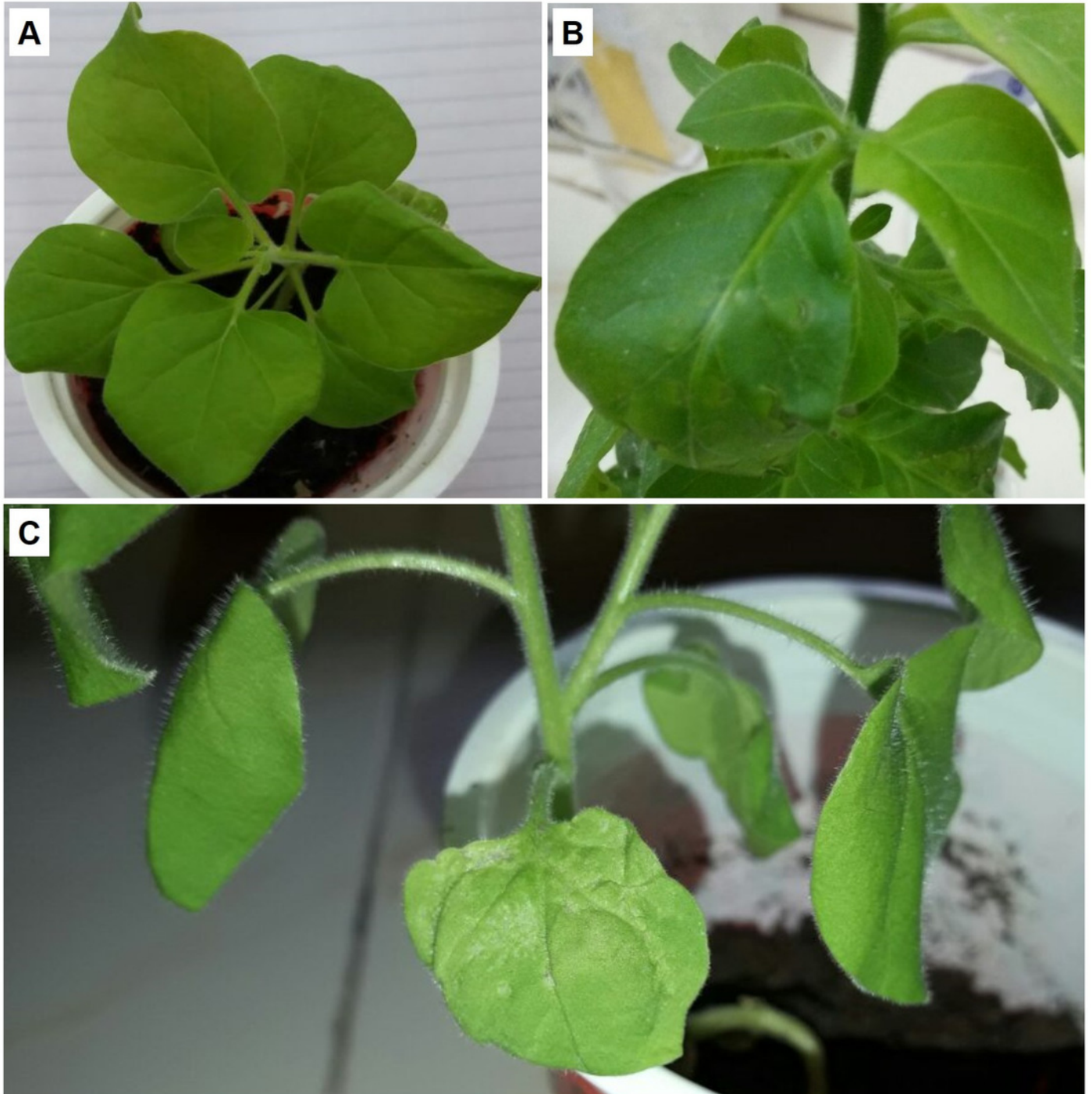
Figure 2

For autoactivation test, few random colonies were patched on SD/-Trp X-α-Gal plates.

βC1 and negative control did not show any autoactivation, positive control turns blue indicating the two proteins interacting.
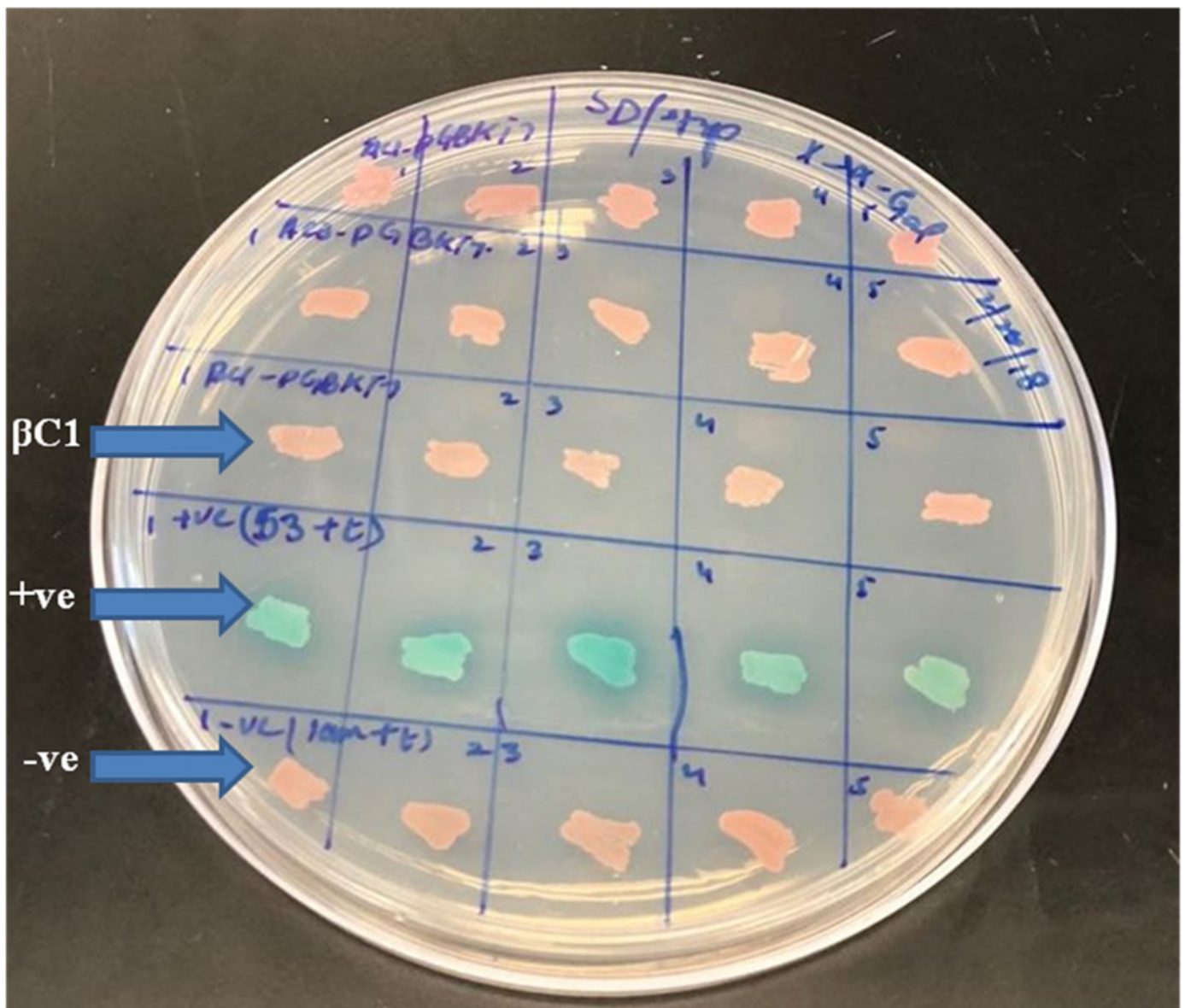
Figure 3

The yeast two hybrid (Y2H) screening using βC1 baits with cDNA library of *Nicotiana benthamiana*

(A) βC1 PCR amplicon on 1% agarose gel, colomn-1 showing 357bp band, colomn-2 showing negative control, colomn-L has 1kb Plus DNA ladder (Thermo Fisher Scietific, USA), (B) Y2H method to identify βC1 interacting proteins, (C) interacting clones (Blue colonies) from 150mm plates patched on DDO/ X-α-Gal plates and QDO/ X-α-Gal plates for the purification.
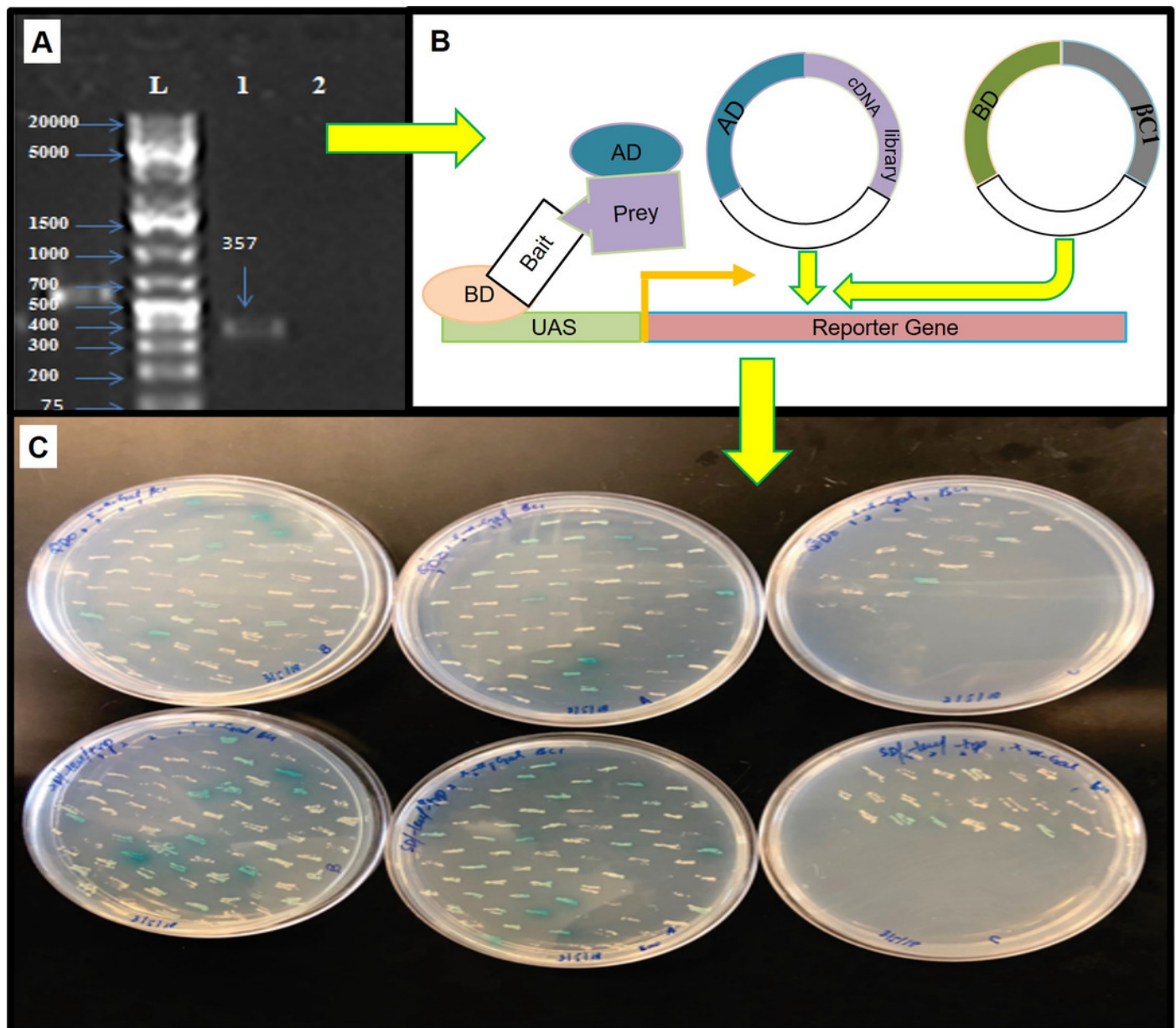
Figure 4

Phylogenetic analysis of NTF2 gene sequence

Showing its close relatives.
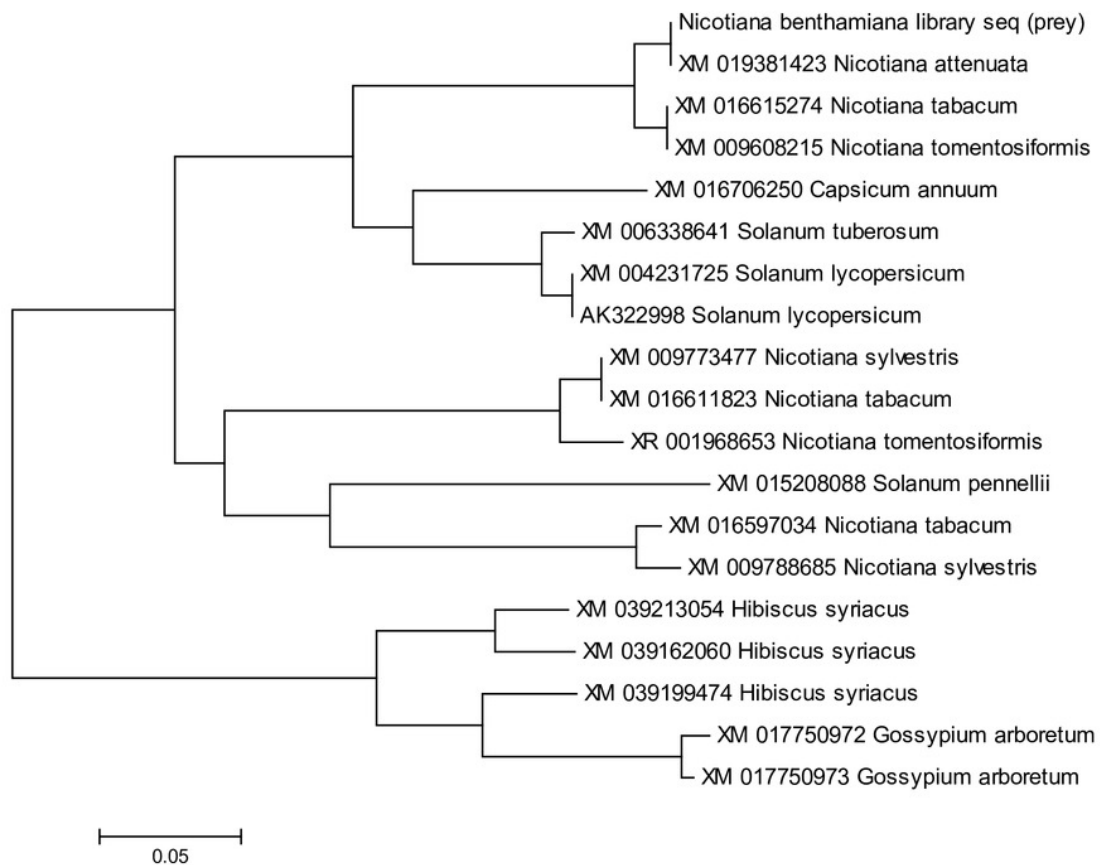
Figure 5

Phylogenetic analysis of NTF2 protein

Showing the close relatives.

Figure 6

Protein primary and secondary structure, and interaction evaluation

(A) Primary Structure analysis of Nuclear Transport Factor2 protein by PortParam with amino acid composition of protein, (B) Secondary Structure analysis of Nuclear Transport Factor2 protein by PRISPRED, (C) Tertiary structure of Nuclear Transport Factor2 protein predicted by I-TASSER, (D) Ramachandran plot, (E) Z-score of NTF2 estimated by Swiss model workspace, (F) Molecular docking complex produced in Cluspro online server showing binding affinity of βC1 with Nuclear Transport Factor2.

Co-transformation scheme of candidate prey with bait and empty bait

Reagents	Selective Agar Plate	Distinct 2mm colonies	Color
Candidate Prey + bait	DDO/X-α-Gal	Yes	Blue
	QDO/X-α-Gal	Yes	Blue
Candidate prey + empty pGBKT7	DDO/X-α-Gal	Yes	White
	QDO/X-α-Gal	No	N/A

The primers used in the study to amplify the activation domain of protein and the targeted genes for sequencing

Name	Sequence
F-AD LD Insert	CTATTCGATGAAGATACCCCACCAAACCC
R-AD LD Insert	GTGAACTTGCGGGGTTTTTCAGTATCTACGATT
SMART III primer	AAGCAGTGGTATCAACGCAGAGTGGCCATTATGGCC
CDS III primer	TCTAGAGGCCGAGGCGGCCGACATG

The dilutions spread on agar plates to determine the mating efficiency, and the number of colonies from each plate with dilution factor1:1000 and 1:10,000

Agar Plate	Dilution Factor	Number of Colonies
	1:1000	>1000
SD/-Trp	1:10,1000	1000
	1:1000	225
SD/-Leu	1:10,1000	53
	1:1000	18
SD/–Leu/–Trp (DDO)	1:10,1000	3

The properties of protein-protein interaction (PPI) including the interacting amino acid residues, and energy released during protein interaction

Property	Description
Interacting Residues of Receptor (βC1 Protein)	TYR48, TYR50, ASP52, ASP58, ASN60
Ligand	NTF2
Interacting Residues of Ligan	GLU38, GLY39, VAL40, PRO56, GLN58, HIS93
Lowest Energy	-730.6 kJ/mol